

Hydrostatic-pressure-induced magnetic structure transformation in polycrystalline $\text{La}_{0.5}\text{Ca}_{0.5}\text{MnO}_{3-\delta}$ ($\delta \leq 0.01$)

Ruiping Wang, Rajappan Mahesh, and Mitsuru Itoh*

Materials and Structures Laboratory, Tokyo Institute of Technology, 4259 Nagatsuta, Midori, Yokohama 226-8503, Japan

(Received 25 January 1999; revised manuscript received 7 July 1999)

Electrical and magnetic properties of $\text{La}_{0.5}\text{Ca}_{0.5}\text{MnO}_{3-\delta}$ ($\delta \leq 0.01$) samples (I, II, III) prepared under different conditions are investigated under varying magnetic fields (0–13 T) and hydrostatic pressures (0 and 13 kbar). All the samples show thermal hysteresis in resistivity. Sample I prepared in oxygen shows antiferromagnetism and insulator behavior at temperatures below the hysteretic region, while sample III prepared in air shows ferromagnetism and metal-like conductivity behavior. Sample II, which is also made in air, shows an intermediate behavior with an unusual insulator-metal transition in the ferromagnetic state. On applying hydrostatic pressure resistivity jumps at low temperatures during cooling and the thermal hysteresis in resistivity increases dramatically on warming for both samples II and III. The origin of anomalous behavior of sample II and III is discussed in terms of coexistence of two magnetic structures and the transformation of the magnetic structure by the application of hydrostatic pressure. [S0163-1829(99)02945-8]

I. INTRODUCTION

Mixed-valent perovskites $\text{Ln}_{1-x}\text{D}_x\text{MnO}_3$, where Ln and D are trivalent rare-earth and divalent-alkaline-earth ions, respectively, show interesting physical properties.^{1–5} These properties can be tuned by controlling several parameters such as doping level (x), A -site average ionic radius ($\langle r_A \rangle$), and so on. For example, in the composition range $0.15 < x < 0.5$, $\text{La}_{1-x}\text{Ca}_x\text{MnO}_3$ exhibits paramagnetic (PM) to ferromagnetic (FM) transition on cooling, accompanied by a sharp drop in the resistivity due to the dominant double-exchange interaction.⁶ When $x > 0.5$, the ground state is antiferromagnetic (AFM) and insulating due to the superexchange interaction between the Mn ions. The behavior corresponding to $x = 0.5$ composition is of particular interest because of the competition between FM double-exchange and AFM superexchange interactions. With decreasing temperature, $\text{La}_{0.5}\text{Ca}_{0.5}\text{MnO}_3$ first undergoes a PM-FM transition around 220 K followed by a simultaneous AFM and charge-ordering (CO) transition near 150 K. The AFM-CO state disappears at 180 K while warming.⁷ The large difference in the AFM-CO transition temperatures between warming and cooling cycles symbols the first-order nature of the CO transition.

It is determined by neutron diffraction that the magnetic structure of $\text{La}_{0.5}\text{Ca}_{0.5}\text{MnO}_3$ is of the charge-exchange (CE)-type.⁸ Along the ac plane ($Pnma$ setting) the Mn^{3+} and Mn^{4+} ions alternate forming $-\text{Mn}^{3+}-\text{O}-\text{Mn}^{4+}-\text{O}-\text{Mn}^{3+}-\text{O}-\text{Mn}^{4+}-$ zigzag chains. The intrachain magnetic spins are ordered ferromagnetically, while the interchain magnetic spins antiferromagnetically. Electron hopping along a chain is impeded by the Coulomb repulsion from the neighboring electrons. This makes the material insulating in the CO state. Recently, Gong *et al.*⁹ have reported unusually high magnetoresistance in $\text{La}_{0.5}\text{Ca}_{0.5}\text{MnO}_3$ in the AFM-CO state. The large value of magnetoresistance was attributed to the field-induced first-order AFM-FM transition. As the canting angle is changed from the AFM phase with

increasing magnetic field, new metastable states have been detected by Xiao *et al.*¹⁰

We have noticed that the low-temperature effective magnetic moments of the $\text{La}_{0.5}\text{Ca}_{0.5}\text{MnO}_3$ samples prepared by them and other groups are much larger than is expected for the AFM phase. Also, the moments at low temperature varied significantly between the reports.^{9,11,12} In certain case the magnetic moment at low temperatures was found to increase with decreasing temperatures at low applied magnetic fields. We considered it worth investigating the low-temperature transport properties of $\text{La}_{0.5}\text{Ca}_{0.5}\text{MnO}_3$ by preparing the samples in different conditions. We found that even slight oxygen nonstoichiometry could dramatically change the low-temperature properties in this system.

II. EXPERIMENT

The samples were prepared by the conventional solid-state reaction method. The raw materials La_2O_3 , CaCO_3 , and MnO_2 were mixed in stoichiometric proportion and calcined at 1273 and 1473 K for over 50 h with intermediate grindings. The resultant powder was pelletized and sintered. Sample I was sintered at 1673 K in flowing oxygen. The sintering temperature for sample II was 1573 K, followed by annealing at 1273 K for 12 h. Sample III was sintered at 1673 K and cooled to room temperature at the rate of 5 K min^{-1} . Calcination and sintering for both samples II and III were carried out in air.

The final product was examined by powder x-ray diffraction using a Mac Science MXP (Ref. 18) x-ray diffractometer with $\text{Cu } K_\alpha$ radiation. Oxygen content was determined by redox titration. Resistivity was measured by the standard four-probe technique under varying magnetic fields (0–13 T) and hydrostatic pressures (0 and 13 kbar). The hydrostatic pressure (P) was generated with a self-clamp-type Cu-Be piston cylinder¹³ and monitored by a manganese resistor. Resistivity under external magnetic field (H) was measured in the following sequence: (1) Cooling the sample to 5 K under zero field. (2) Applying field to the selected value. (3) Field

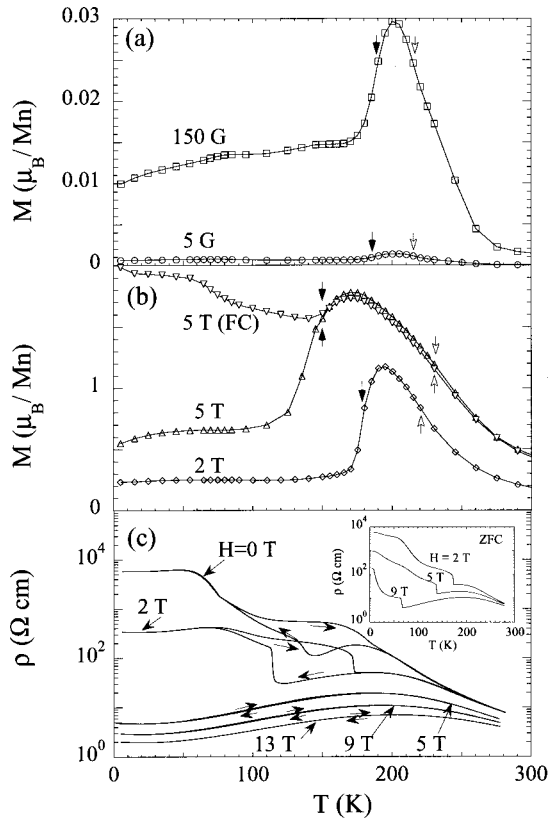


FIG. 1. The temperature variation of (a) magnetic moment under 5 and 150 G, (b) magnetic moment under 2 T, 5 T (ZFC and FC), and (c) resistivity of sample II under varying magnetic fields. Inset shows the resistivity data recorded on warming after zero-field cooling. Open and filled arrows in (a) and (b) indicate T_C and T_N , respectively.

warming to 280 K. (4) Field cooling to 5 K. (5) Field warming to 280 K again. Magnetic measurements were carried out using a Quantum Design magnetic property measurement system (MPMS) superconducting quantum interference device (SQUID) magnetometer. Both zero-field-cooling (ZFC) and field-cooling (FC) data were recorded during warming run.

III. RESULTS AND DISCUSSION

X-ray-diffraction profiles show that all the three samples are single-phase orthorhombic perovskites with space group $Pnma$. Oxygen deficiencies (δ) of all the three samples are determined by redox titration method to be less than 1%. So the gross ratio of Mn^{3+}/Mn^{4+} is 1:1. The resistivity behavior of sample I agrees well with the earlier reports⁷ on $La_{0.5}Ca_{0.5}MnO_3$. Sample II as well as sample III also exhibits a thermal hysteresis in resistivity indicative of first-order transition arising from charge ordering. However, several unusual features are obvious.

Temperature variation of magnetic moment (M) and resistivity (ρ) for sample II is shown in Fig. 1. On cooling, sample II undergoes PM-FM transition at $T_C = 220$ K and FM-AFM transition at $T_N = 185$ K [Fig. 1(a)]. The AFM transition is shifted to lower temperature by external magnetic field [Figs. 1(a) and 1(b)]. ρ exhibits semiconductorlike behavior at both high-temperature range ($T > 170$ K) and

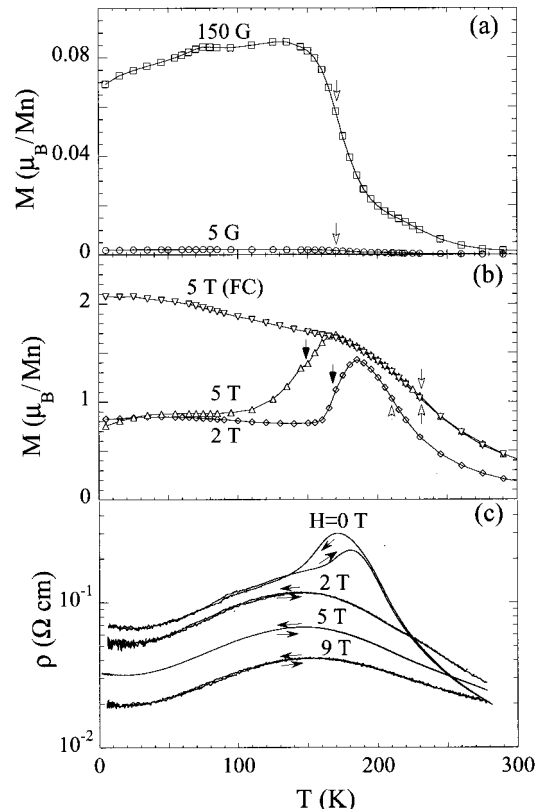


FIG. 2. The temperature variation of (a) magnetic moment under 5 and 150 G, (b) magnetic moment under 2 T, 5 T (ZFC and FC), and (c) resistivity of sample III under varying magnetic fields. Open and filled arrows in (a) and (b) indicate T_C and T_N , respectively.

low-temperature range ($T < 140$ K). Whereas, on cooling and within temperature range 140–170 K, unusual metal-like variation is observed. Hysteresis in resistivity vanishes under the 13-T field on ZFC and under 9-T field on FC, implying the complete suppression of the CO state. As a result of the gradual suppression of the CO state, resistivity decreases drastically with increasing field. Magnetoresistance [defined as $[\rho(0) - \rho(H)]/\rho(0)$] reaches $\sim 90\%$ around 175 K just with 2-T field.

Under magnetic fields lower than 150 G, sample III shows PM-FM transition only [Fig. 2(a)]. No FM-AFM transition is observed. However, when fields higher than 2 T are applied, the FM-AFM transition appears [Fig. 2(b)]. The transition shifts to low temperatures with increasing fields and is completely suppressed by a 5-T magnetic field on FC. Contrary to sample II, sample III shows higher magnetic moment and metal-like resistivity behavior at low temperatures.

The effects of hydrostatic pressure on the resistivity of sample II and III are shown in Figs. 3(a) and 3(b), respectively. The data obtained under 0 kbar and 0 T are given in broken line for comparison and the ZFC data for sample II is given in the inset of Fig. 3(a). For sample II, on applying 13-kbar hydrostatic pressure, a sharper AFM-CO transition, an enhanced hysteresis and a resistivity jump around 80 K during cooling is observed. Like under ambient pressure, magnetic fields suppress the hysteresis and shift AFM-CO transition to low temperatures. For sample III, under 13-kbar pressure and 0-T field, ρ increases with decreasing temperature first, and then a jump around 50 K appears while cool-

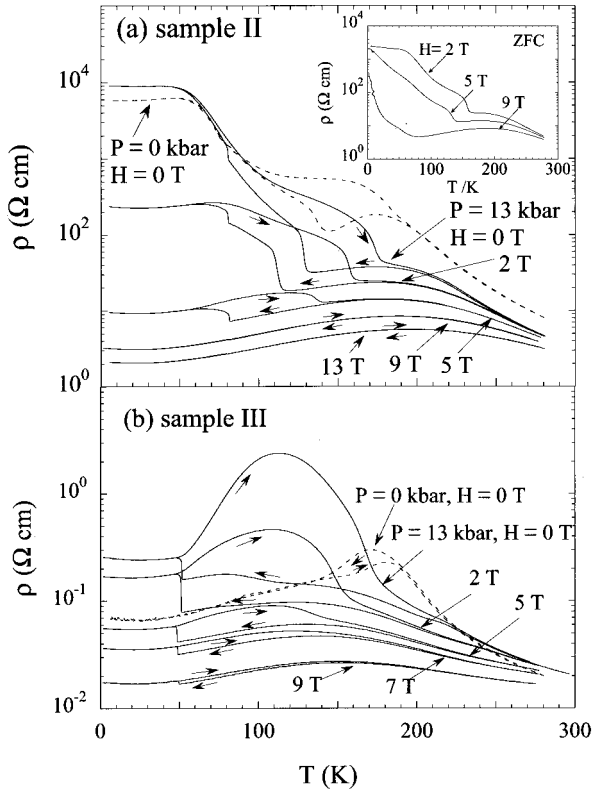


FIG. 3. The temperature variation of resistivities of (a) sample II, (b) sample III under 13-kbar hydrostatic pressure and varying magnetic fields. Resistivity data obtained under ambient pressure and 0 T are shown by broken lines for comparison. Inset shows the resistivity data recorded on warming after zero-field cooling.

ing. During warming, ρ increases steeply at 50 K, reaches a maximum around 115 K, and decreases with a change in slope around 180 K. Compared to the result under ambient pressure, the hysteresis is drastically enhanced. The enhanced hysteresis is suppressed by external magnetic fields progressively, but remains visible to the maximum applied magnetic field of 9 T.

It is noticed that the low-temperature magnetic moment of three samples varies in the order of $M_I < M_{II} < M_{III}$. The lower the oxygen partial pressure when sintering and/or the shorter the annealing time after sintering is, the higher the M is. As both low-oxygen partial pressure and short annealing time tend to make oxygen nonstoichiometric, the low-temperature magnetic moment is evidently related to oxygen off stoichiometry. We have annealed sample III in flowing oxygen for 24 h and found that the oxygenated sample III showed similar properties as that of stoichiometric $\text{La}_{0.5}\text{Ca}_{0.5}\text{MnO}_3$. The low-melting field of CO for sample III (5 T, FC) and the high magnetoresistance under low magnetic field for sample II ($\sim 90\%$ around 175 K with 2-T field) also favor the oxygen off stoichiometry ($\delta \leq 0.01$) in the samples.¹⁴

According to the double-exchange model, the effective-transfer integral t of the e_g carrier is expressed as

$$t = t_0 \cos(\Delta\theta/2),$$

where t_0 is the bare transfer integral without spin scattering and $\Delta\theta$ is the relative angle of the neighboring t_{2g} spins. The

external pressure increases t_0 via volume contraction. CO is suppressed by the pressure-enhanced carrier itinerancy. The effects of pressure on the CO transition are reported almost equivalent to that due to magnetic field: shifting T_{CO} to low-temperature and depressing hysteresis.¹⁵ However, in the present study, magnetic field and hydrostatic pressure are found to have opposite effects on CO. Rather than being suppressed, hysteresis is enhanced by hydrostatic pressure. The fact suggests that, other than the double-exchange interaction, there must be additional mechanisms that are responsible for the unusual behavior of samples II and III under hydrostatic pressure.

Earlier research reveals that transport properties of manganates are closely related to the magnetic structure of samples. $\text{Pr}_{0.5}\text{Sr}_{0.5}\text{MnO}_3$, resembling to $\text{La}_{0.5}\text{Ca}_{0.5}\text{MnO}_3$, undergoes a PM-FM transition at high temperature and a FM-AFM transition at low temperature, too.⁴ The magnetic structure for $\text{Pr}_{0.5}\text{Sr}_{0.5}\text{MnO}_3$ sample prepared in oxygen is reported to be of CE-type and the CO occurs simultaneously with the FM-AFM transition.¹⁶ Whereas the magnetic structure for the $\text{Pr}_{0.5}\text{Sr}_{0.5}\text{MnO}_3$ sample prepared in air is reported to be of A type, the CO is absent and resistivity is fairly low ($\sim 10^{-2} \Omega \text{ cm}$) even around 5 K. The different magnetic structure is attributed to a slight off-stoichiometry (different x and/or oxygen content) between the samples.¹⁷

Neutron-diffraction experiment reveals that for the $\text{La}_{1-x}\text{Ca}_x\text{MnO}_3$ ($0 \leq x \leq 1$) system, magnetic structure varies according to the doping region. In some doping regions, two magnetic structures could coexist.⁸ Careful synchrotron x-ray-diffraction found that in $\text{Nd}_{0.5}\text{Sr}_{0.5}\text{MnO}_3$, the FM state, the CO state, and probably the orbitally ordered state coexist around $T_{\text{CO}} = 150$ K. At low temperatures ($T \ll T_{\text{CO}}$), a small fraction of the FM state persists along with the CO and orbitally ordered phases.²⁰ Since three samples have the same charge-carrier density, stimulated by the above-mentioned experiment results on half-doped ($x = 0.5$) manganates, we consider the anomalous behavior of the samples II and III at low temperatures to have relation with magnetic inhomogeneity. The fairly low-resistivity value ($\sim 7 \times 10^{-2} \Omega \text{ cm}$) and the relative high-magnetic moment ($\sim 0.07 \mu_B$ /per Mn under 150 G) of sample III at low temperatures suggest that the dominant low-temperature magnetic structure for it is different from that for stoichiometric $\text{La}_{0.5}\text{Ca}_{0.5}\text{MnO}_3$ (CE type). It is a magnetic structure with stronger ferromagnetic interaction. Noticing the preparation atmosphere, we speculate that, similar to the $\text{Pr}_{0.5}\text{Sr}_{0.5}\text{MnO}_3$ sample prepared in air, the dominant phase for sample III is of A-type magnetic structure and charge disordered.¹⁸ The high resistivity of sample II around 5 K suggests that the dominant magnetic structure for it is still of CE type. But the intermediate resistivity behavior hints the existence of another magnetic structure (may be of A type) to some extent.

According to the discussions above, we suggest the following explanations for our experiment results. Samples II and III are subtle oxygen nonstoichiometric. Slight oxygen nonstoichiometry causes the coexistence of two phases in the samples. One phase is of A-type magnetic structure and charge disordered (phase I) and the second phase is of CE-type magnetic structure and charge ordered (phase II). Physical properties are governed by the dominant phase. In sample III, phase I dominates. So, it shows metal-like resistivity be-

havior and high-magnetic moment at low temperatures. Sample II, which is dominated by phase II, shows similar behavior like that of stoichiometric $\text{La}_{0.5}\text{Ca}_{0.5}\text{MnO}_3$. However, phase I manifests itself via the anomalous $d\rho/dT > 0$ range while cooling and the almost constant ρ below 60 K. On applying hydrostatic pressure, the *A*-type magnetic structure is transformed to CE type. The resistivity jump around 50 K for sample III during cooling corresponds to the transformation of magnetic structure. The low ρ after the transformation ($T < 50$ K) implies that charges still remain in the disordered state, probably because the temperature is too low and carriers do not have enough energy to move. On warming to above 50 K, thermal energy helps carriers to move and CO occurs. Consequently, ρ increases dramatically and an enhanced hysteresis is observed. The slope change at 180 K during warming evidences the disappearance of the CO state.¹⁹ The same is true for sample II. The resistivity jump around 80 K during cooling under 13-kbar pressure and enhanced hysteresis are evidences of the transformation of the *A*-type magnetic structure to CE-type magnetic structure. As in the case of other manganates,²⁰ magnetic field melts the CO state and the hysteresis in resistivity is suppressed (Fig. 3).

For half-doped manganates, the layered *A*-type AFM structure is favored by a wide one-electron bandwidth (W).¹⁷ On increasing W via the application of hydrostatic pressure, a transformation of the CE-type magnetic structure to *A*-type magnetic structure was reported in polycrystalline $(\text{Nd}_{1-y}\text{La}_y)_{1/2}\text{Sr}_{1/2}\text{MnO}_3$ ($y = 0.4$).¹⁵ On the contrary to the above results, in the present study, a pressure-induced *A*-type

to CE-type magnetic structure transformation was observed. The apparent contradiction could mean that, for a half-doped manganate, the balance between the ferromagnetic double-exchange and the antiferromagnetic superexchange interactions is very sensitive to even extremely low-oxygen deficiencies ($\delta \leq 0.01$). To describe the half-doped manganates fully, it is necessary to take δ as one of the independent parameters.

IV. CONCLUSIONS

We have examined the electrical and magnetic properties of three $\text{La}_{0.5}\text{Ca}_{0.5}\text{MnO}_{3-\delta}$ samples prepared under different conditions. It is found that two phases, which are due to slight oxygen off stoichiometry, coexist in samples II and III. A hydrostatic-pressure-induced CO and magnetic structure transformation (*A* type to CE type) are observed. The present study suggests that the competition between the ferromagnetic double-exchange and the antiferromagnetic superexchange interactions is sensitive to even slight oxygen off stoichiometry.

ACKNOWLEDGMENTS

Part of this work was financially supported by JSPS research for the Future Program in the Area of Atomic-Scale Surface and Interface Dynamics and a Grant-in-Aid for Scientific Research from Ministry of Education, Science, and Culture.

*Author to whom correspondence should be addressed. Electronic address: m.itoh@rlem.titech.ac.jp

¹S. Jin, T. H. Tiefel, M. McCormack, R. A. Fastnacht, R. Ramesh, and L. H. Chen, *Science* **264**, 413 (1994).

²Y. Tomioka, A. Asamitsu, Y. Moritomo, H. Kuwahara, and Y. Tokura, *Phys. Rev. Lett.* **74**, 5108 (1995).

³V. Kiryukhin, D. Casa, J. P. Hill, B. Keimer, A. Vigliante, Y. Tomioka, and Y. Tokura, *Nature (London)* **386**, 813 (1997).

⁴J. Barratt, M. R. Lees, G. Balakrishnan, and D. McK Paul, *Appl. Phys. Lett.* **68**, 424 (1996).

⁵A. Asamitsu, Y. Moritomo, R. Kumai, Y. Tomioka, and Y. Tokura, *Phys. Rev. B* **54**, 1716 (1996).

⁶C. Zener, *Phys. Rev.* **82**, 403 (1951).

⁷A. P. Ramirez, P. Schiffer, S.-W. Cheong, C. H. Chen, W. Bao, T. T. M. Palstra, P. L. Gammel, D. J. Bishop, and B. Zegarski, *Phys. Rev. Lett.* **76**, 3188 (1996).

⁸E. O. Wollan and W. C. Koehler, *Phys. Rev.* **100**, 545 (1955); John B. Goodenough, *ibid.* **100**, 564 (1955); P. G. Radaelli, D. E. Cox, M. Marezio, and S.-W. Cheong, *Phys. Rev. B* **55**, 3015 (1997).

⁹G. Q. Gong, C. L. Canedy, and Gang Xiao, *J. Appl. Phys.* **79**, 4538 (1996).

¹⁰Gang Xiao, G. Q. Gong, C. L. Canedy, E. J. McNiff, and A.

Gupta, *J. Appl. Phys.* **81**, 5324 (1997).

¹¹P. G. Radaelli, D. E. Cox, M. Marezio, S.-W. Cheong, P. E. Schiffer, and A. P. Ramirez, *Phys. Rev. Lett.* **75**, 4488 (1995).

¹²C. H. Booth, F. Bridges, G. J. Snyder, and T. H. Geballe, *Phys. Rev. B* **54**, R15 606 (1996).

¹³T. Huang, M. Itoh, J. D. Yu, Y. Inaguma, and T. Nakamura, *Phys. Rev. B* **48**, 7712 (1993).

¹⁴M. Tokunaga, N. Miura, Y. Tomioka, and Y. Tokura, *Phys. Rev. B* **57**, 5259 (1998).

¹⁵Y. Moritomo, H. Kuwahara, Y. Tomioka, and Y. Tokura, *Phys. Rev. B* **55**, 7549 (1997).

¹⁶K. Knizek, Z. Jirak, E. Pollert, F. Zounova, and S. Vratilav, *J. Solid State Chem.* **100**, 292 (1992).

¹⁷H. Kawano, R. Kajimoto, H. Yoshizawa, Y. Tomioka, H. Kuwahara, and Y. Tokura, *Phys. Rev. Lett.* **78**, 4253 (1997).

¹⁸The hysteresis in Fig. 1(c) may be due to the minor phase that of CE-type magnetic structure and with charge ordering.

¹⁹Our ac susceptibility measurement of sample I under 8-kbar hydrostatic pressure shows that the CO transition temperature is almost unaffected.

²⁰C. N. R. Rao, Anthony Arulraj, P. N. Santosh, and A. K. Cheetham, *Chem. Mater.* **10**, 2714 (1998).